Supporting Information

Synthesis and Properties of Unsymmetrical Azatrioxa[8]circulenes

Malene Plesner,[a] Thomas Hensel,[a] Bjarne E. Nielsen,[a] Fadhil S. Kamounah,[a] Theis Brock-Nannestad,[a] Christian B. Nielsen,[a] Christian G. Tortzen, Ole Hammerich,[a] and Michael Pittelkow[a*]

University of Copenhagen, Department of Chemistry, Universitetsparken 5, DK-2100, Copenhagen Ø, Denmark;
Tel: 0045 35320155; E-mail: pittel@kiku.dk

Contents

S1 General

All chemicals and solvents, unless otherwise stated, were purchased from commercial suppliers and used as received. Analytical thin layer chromatography (TLC) was performed on SiO_2 60F254 plates purchased from Merck and visualized under UV-light (254 or 360 nm). Dry column vacuum chromatography was carried out using SiO_2 from ROCC (SI 1722, 60 Å, 15 – 40 μm).

NMR spectra were recorded on a Bruker Ultrashield Plus 500 MHz spectrometer. Temperature dependent NMR spectra were recorded on a Varian 300 MHz spectrometer. ^1H NMR and ^{13}C NMR spectra were recorded at 500 MHz and 125 MHz, respectively, on a Bruker Ultrashield Plus 500 spectrometer using residual non-deuterated solvent as the internal standard. All chemical shifts (δ) are quoted in ppm and all coupling constants (J) are expressed in Hertz (Hz). The following abbreviations are used for convenience in reporting the multiplicity for NMR resonances: s = singlet, bs = broad singlet, d = doublet, t = triplet, q = quartet, and m = multiplet. Samples were prepared using $CDCl_3$ or DMSO-d_6 purchased from Euriso-Top or Cambridge Isotope Labs, respectively. The NMR data was processed using MestReNova v. 8.0.2. Assignment of all ^1H and ^{13}C resonances was achieved using standard 2D NMR techniques as ^1H-^1H COSY, ^1H-^{13}C HSQC, and ^1H-^{13}C HMBC.

Melting points were obtained on a Stuart SMP3 apparatus.

Elemental analysis was conducted at the Microanalytical Laboratory, at the Department of Chemistry, University of Copenhagen.

MALDI-TOF MS was recorded on a Bruker Autoflex apparatus using dithranol as matrix. MALDI HRMS was recorded on a Bruker Solarix ESI/MALDI FTMS instrument, dithranol was used as matrix, and calibration was performed externally, using sodium trifluoroacetate cluster ions. Gas chromatography mass spectrometry (GC-MS) was recorded on an Agilent 6890 Series GC-system combined with a Agilent 5973N mass selective detector.

UV-Vis measurements were done on a Cary 5E UV-Vis-NIR spectrophotometer and Fluorescence was measured using a Perkin Elmer Luminescence Spectrometer LS50B.

Cyclic voltammetry was carried out using an Autolab PGSTAT12 or an CH Instruments CHI400A system, using, unless otherwise stated, a sample concentration of approx. $5 \cdot 10^{-4}$ mol·L^{-1}. $(n\mathrm{Bu})_4NPF_6$ (1M) was used as supporting electrolyte. The working electrode was a circular glassy carbon disk (d

= 3 mm) . A Pt-wire served as the counter electrode and the reference electrode was Ag/Ag^+. The potential scale was subsequently calibrated by recording the potential of the ferrocene/ferrocenium redox couple.The voltage sweep rate was 0.1 V s^{-1} and all experiments were carried out at room temperature unless otherwise stated.

S2 Computational details

The geometry optimization was performed by the DFT B3LYP/6-31G(d) level using the GAUSSIAN 03 package.

Based on the calculated coordinates of the ring critical points of the (3, +1) type the NICS (0) and NICS(1) indices are calculated by the B3LYP/6-311+G(d,p) level with the gauge-independent atomic orbital (GIAO) approach. Negative NICS values in the center of the ring corresponds to the presence of the “aromatic” diatropic ring currents, whereas positive NICS values at the same points denote the “antiaromatic” paratropic ring currents.

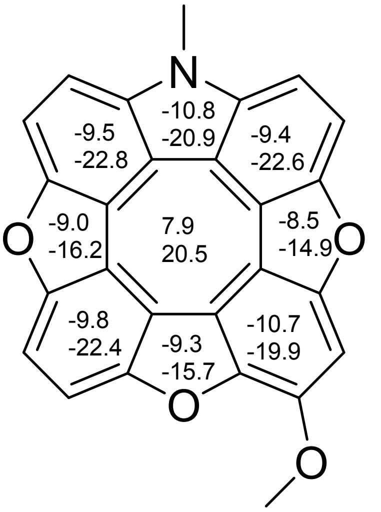

Fig. S1. NICS(0) and $NICS(1)_{zz}$ (lower numbers) values calculated for the methoxy substituted azatrioxa[8]circulene (**2**).

```
SCF Done:  E(RB3LYP) =  -1317.06048693, Number of imaginary frequencies: 0

---------------------------------------------------------------------
 Center     Atomic      Atomic             Coordinates (Angstroms)
 Number     Number       Type              X           Y           Z
 ---------------------------------------------------------------------
      1          6           0       -2.796616   -1.898015   -0.009019
      2          6           0       -2.708237   -3.302599    0.002008
      3          6           0       -1.640031   -1.078049   -0.005341
      4          6           0       -1.448868   -3.905234    0.004067
      5          6           0       -0.379509   -1.686029   -0.004357
      6          6           0       -0.320772   -3.081029   -0.000571
      7          6           0       -0.127144    3.384290    0.001400
      8          6           0       -0.061521    1.963224   -0.001870
      9          6           0        0.987745    4.211861    0.003366
     10          6           0        1.194645    1.374777   -0.002167
     11          6           0        2.245692    3.588598    0.002193
     12          6           0        2.356279    2.191156   -0.000202
     13          6           0        3.606193    1.403074   -0.000953
     14          6           0        0.994115   -1.225124   -0.001958
     15          6           0        1.787372   -2.418883    0.001104
     16          6           0        1.663017   -0.023218   -0.002345
     17          6           0        3.159923   -2.431731    0.002792
     18          6           0        3.103480    0.035522   -0.000602
     19          6           0        3.838468   -1.180085    0.001399
     20          8           0        0.994153   -3.535080    0.002430
     21          8           0       -1.429666    3.817930    0.002717
     22          6           0       -4.269967    1.435499    0.002177
     23          6           0       -3.505184    0.252355   -0.008720
     24          6           0       -3.617525    2.668380    0.004319
```

25	6	0	-2.089376	0.280811	-0.005162
26	6	0	-2.218515	2.678055	-0.000315
27	6	0	-1.438078	1.519672	-0.004103
28	7	0	-3.922591	-1.077277	-0.028393
29	6	0	-5.296565	-1.529815	0.022537
30	8	0	5.172082	-1.314593	0.003015
31	6	0	6.052795	-0.183883	0.000330
32	1	0	0.878828	5.291039	0.005752
33	1	0	3.152790	4.185827	0.003584
34	1	0	7.055094	-0.618805	0.002458
35	1	0	5.886114	0.444344	0.877787
36	1	0	5.887742	0.438670	-0.881506
37	1	0	3.731095	-3.352165	0.004991
38	1	0	-1.345000	-4.984722	0.013178
39	1	0	-3.598854	-3.922662	0.014929
40	1	0	-5.385003	-2.491597	-0.489407
41	1	0	-5.658670	-1.642839	1.053043
42	1	0	-5.937653	-0.814751	-0.499761
43	1	0	-5.354734	1.403629	0.014895
44	1	0	-4.177052	3.597430	0.013455

S3 Characterisation Data

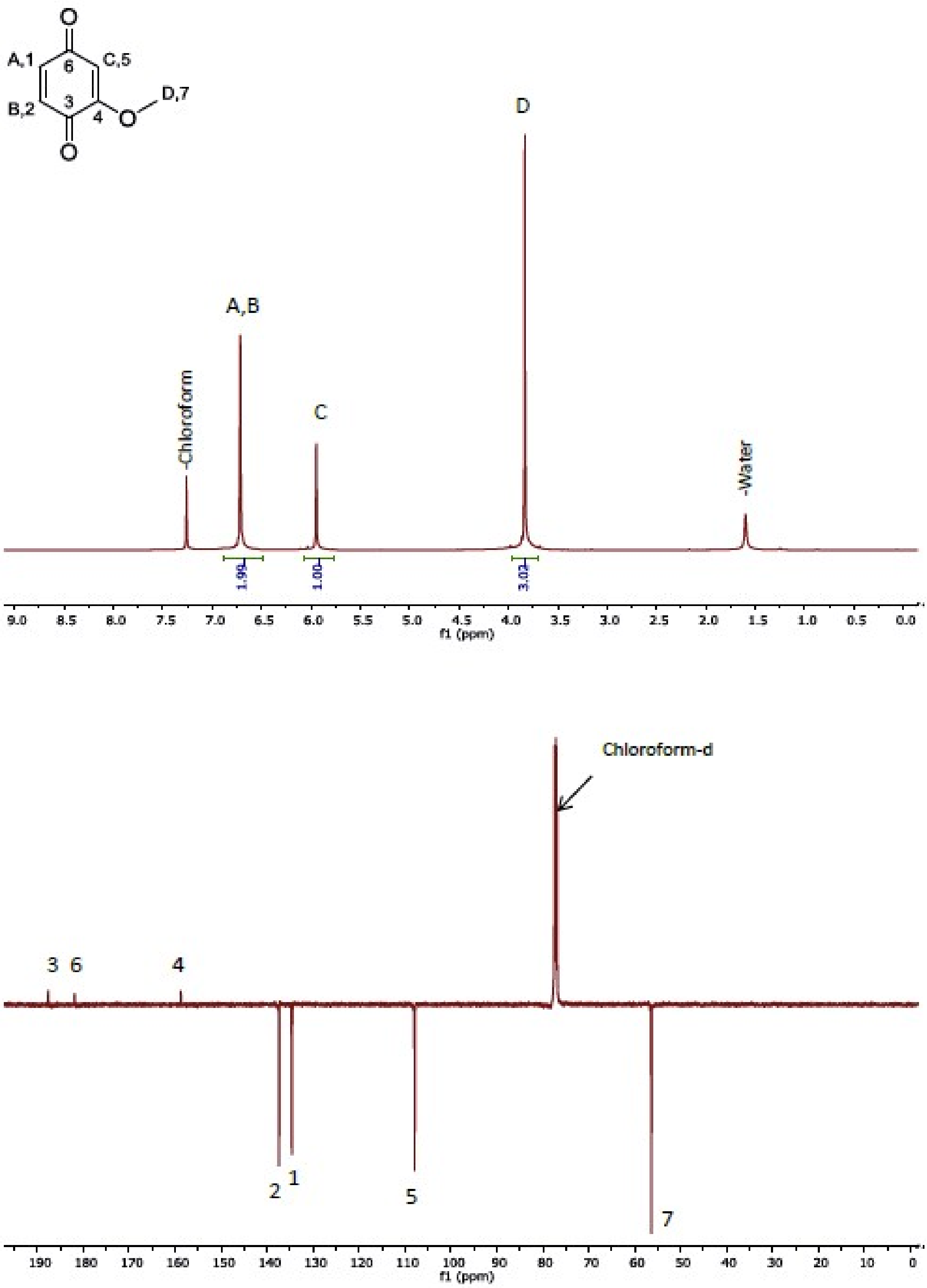

Fig. S3.0: ^{1}H and ^{13}C NMR spectra of 2-methoxy-benzoquinone.

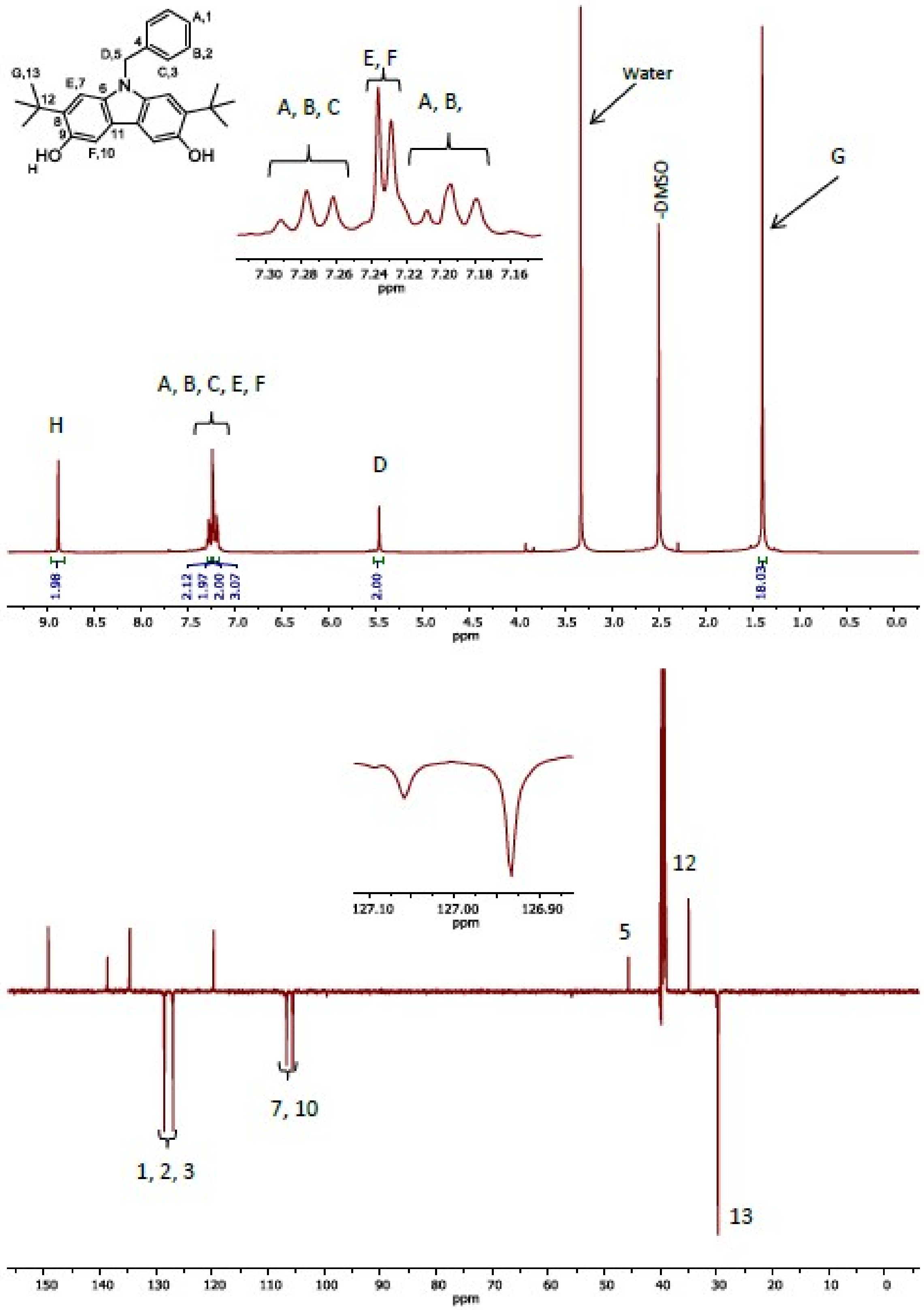

Fig. S3.1: ^{1}H and ^{13}C NMR spectra of compound **4**.

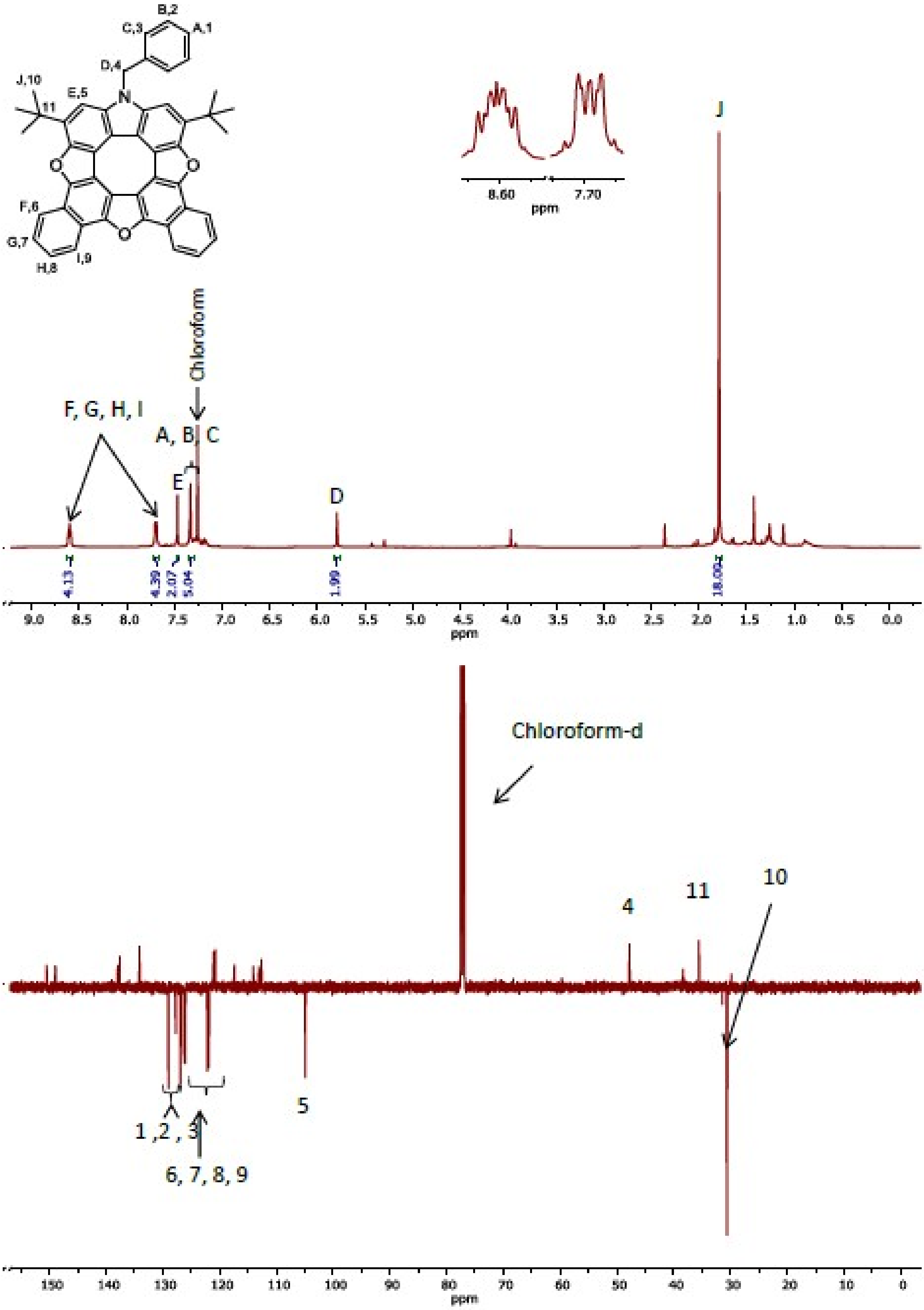

Fig. S3.2: ^{1}H and ^{13}C NMR spectra of compound $\mathbf{2}_{\mathbf{PhePhe}}$.

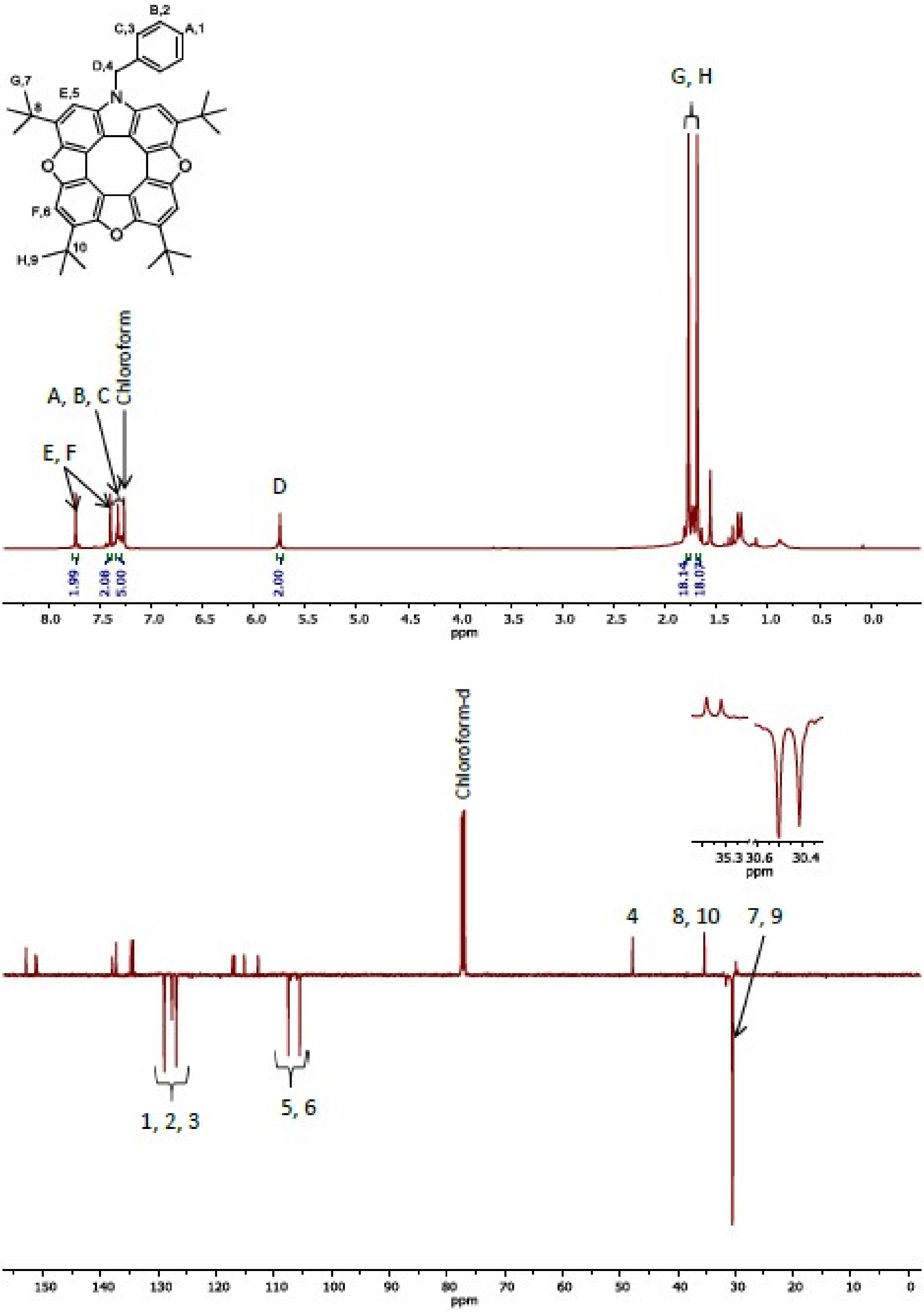

Fig. S3.3: ^{1}H and ^{13}C NMR spectra of compound $\mathbf{2}_{\boldsymbol{t}\mathbf{Bu}\boldsymbol{t}\mathbf{Bu}}$.

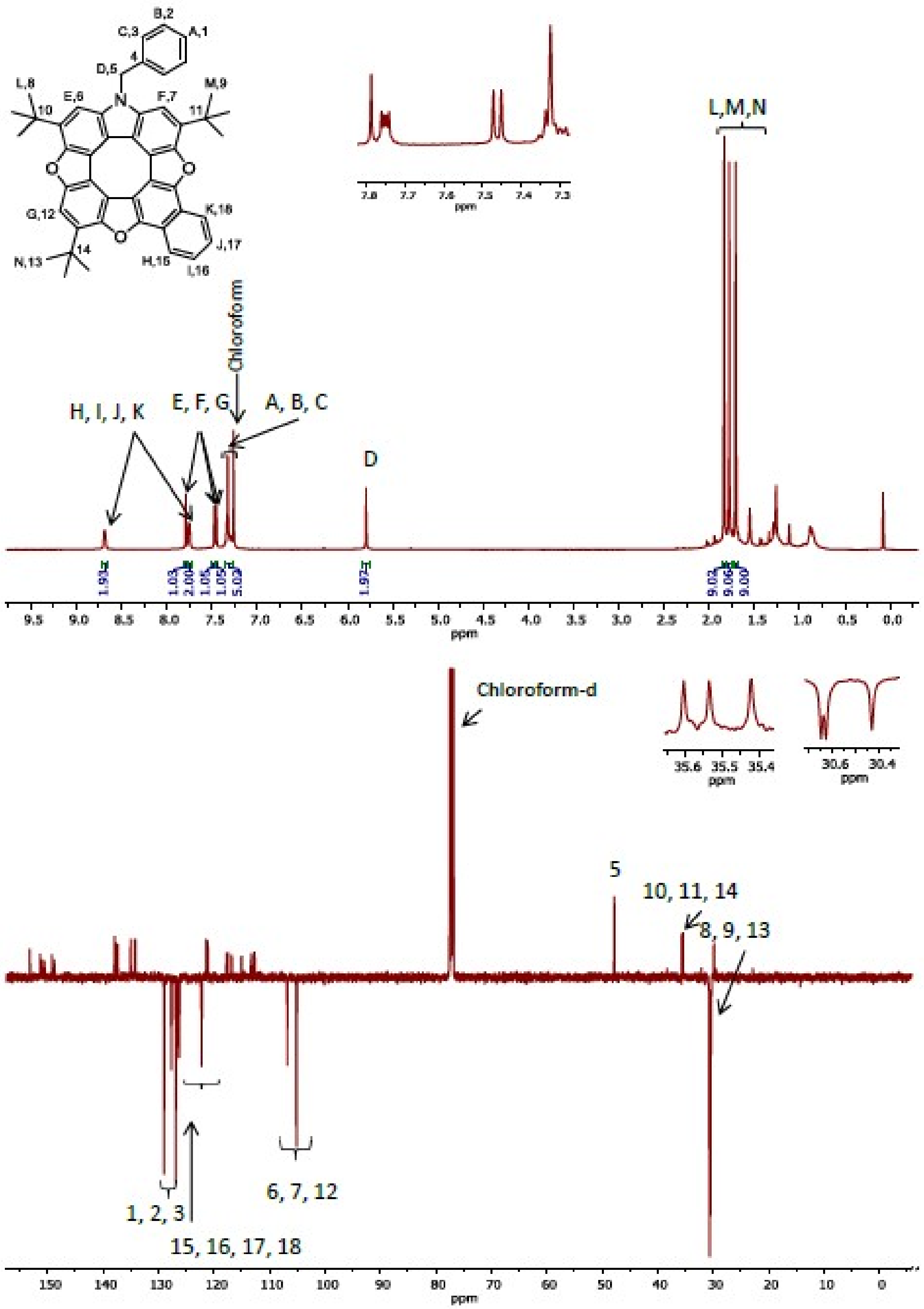

Fig. S3.4: ^{1}H and ^{13}C NMR spectra of compound $\mathbf{2}_{\boldsymbol{t}\mathbf{BuPhe}}$.

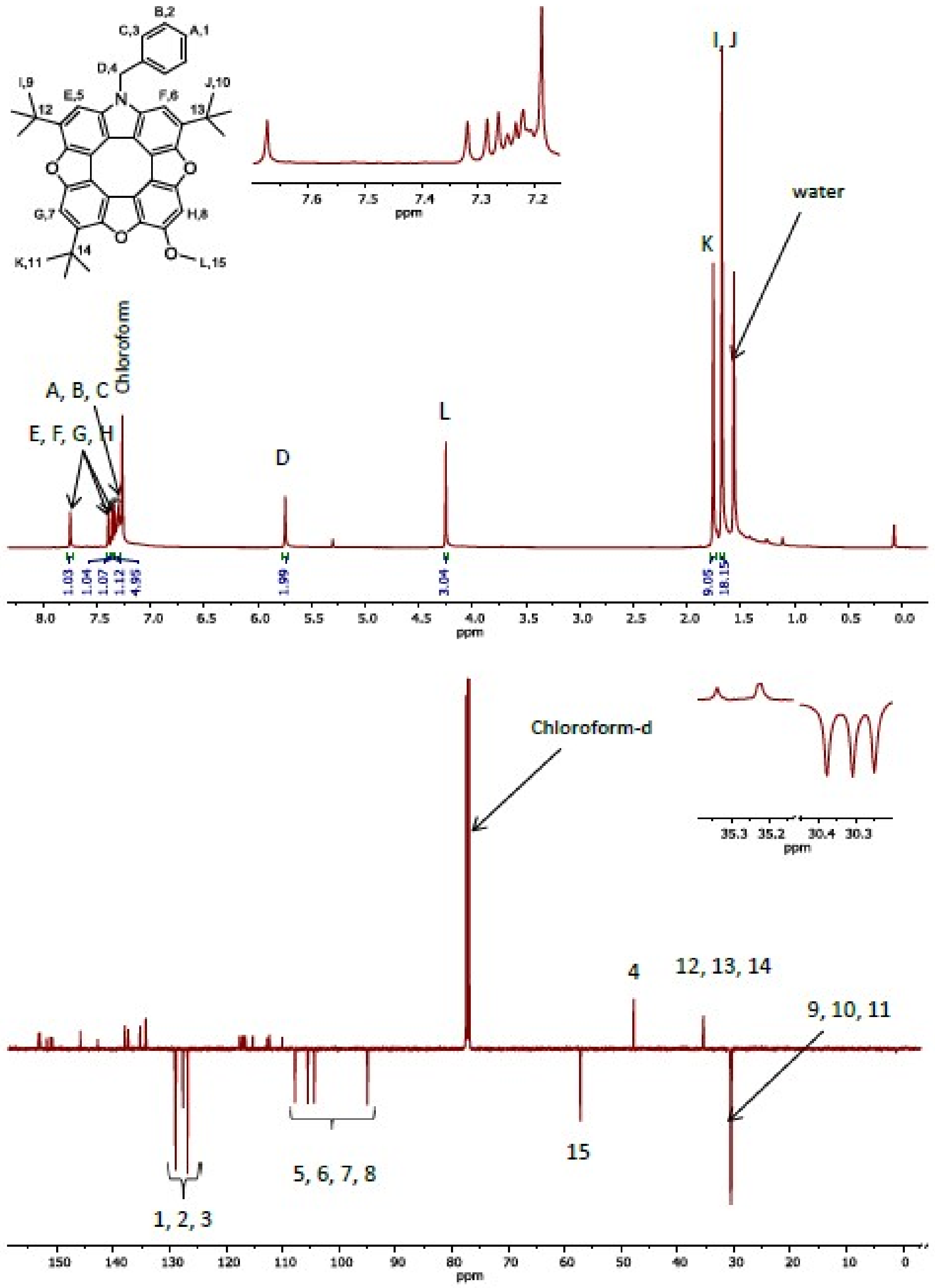

Fig. S3.5: ^{1}H and ^{13}C NMR spectra of compound **2**$_{\mathbf{\mathit{t}BuOMe}}$.

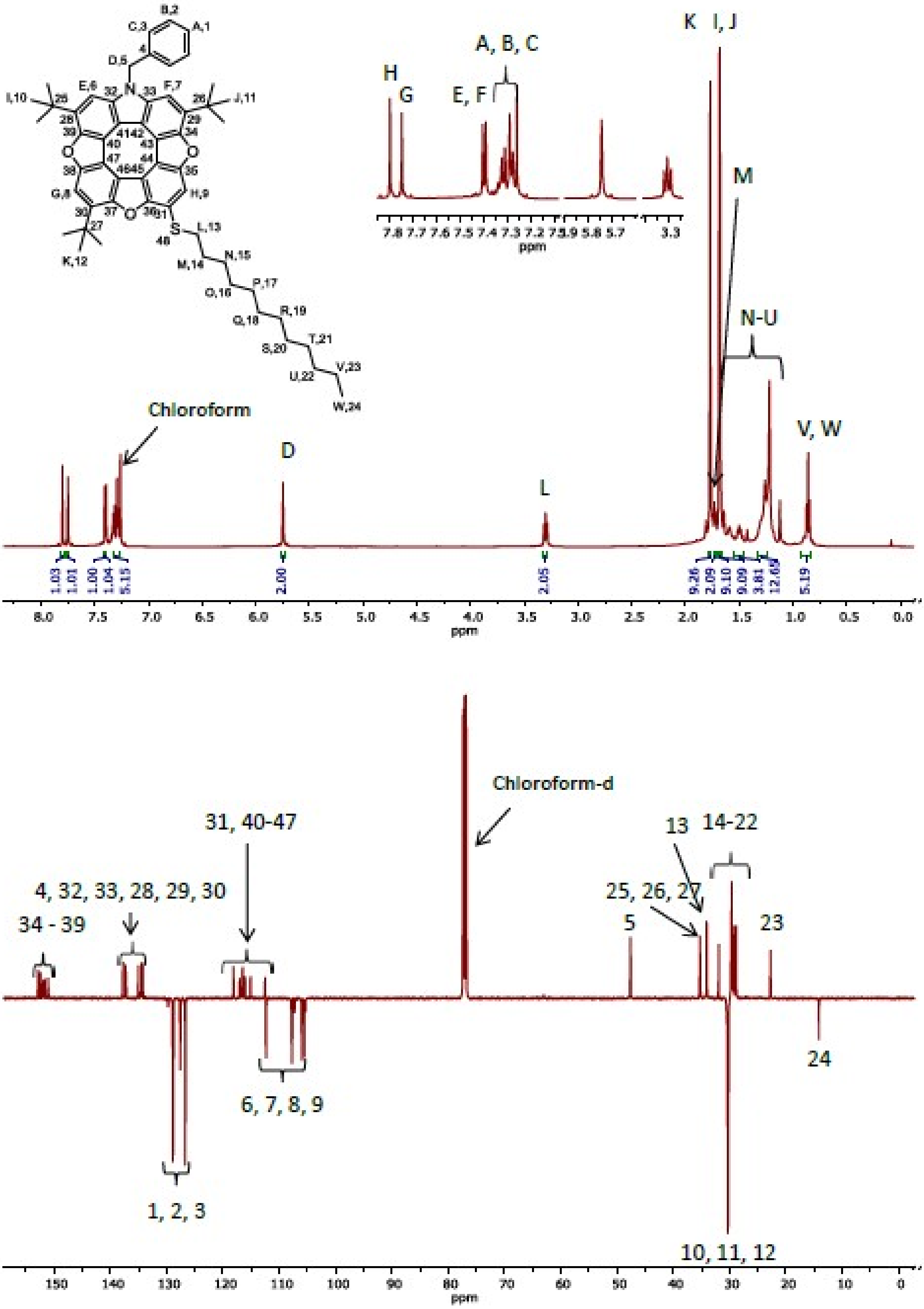

Fig. S3.6: ^{1}H and ^{13}C NMR spectra of compound **$2_{t\text{BuSDo}}$**.

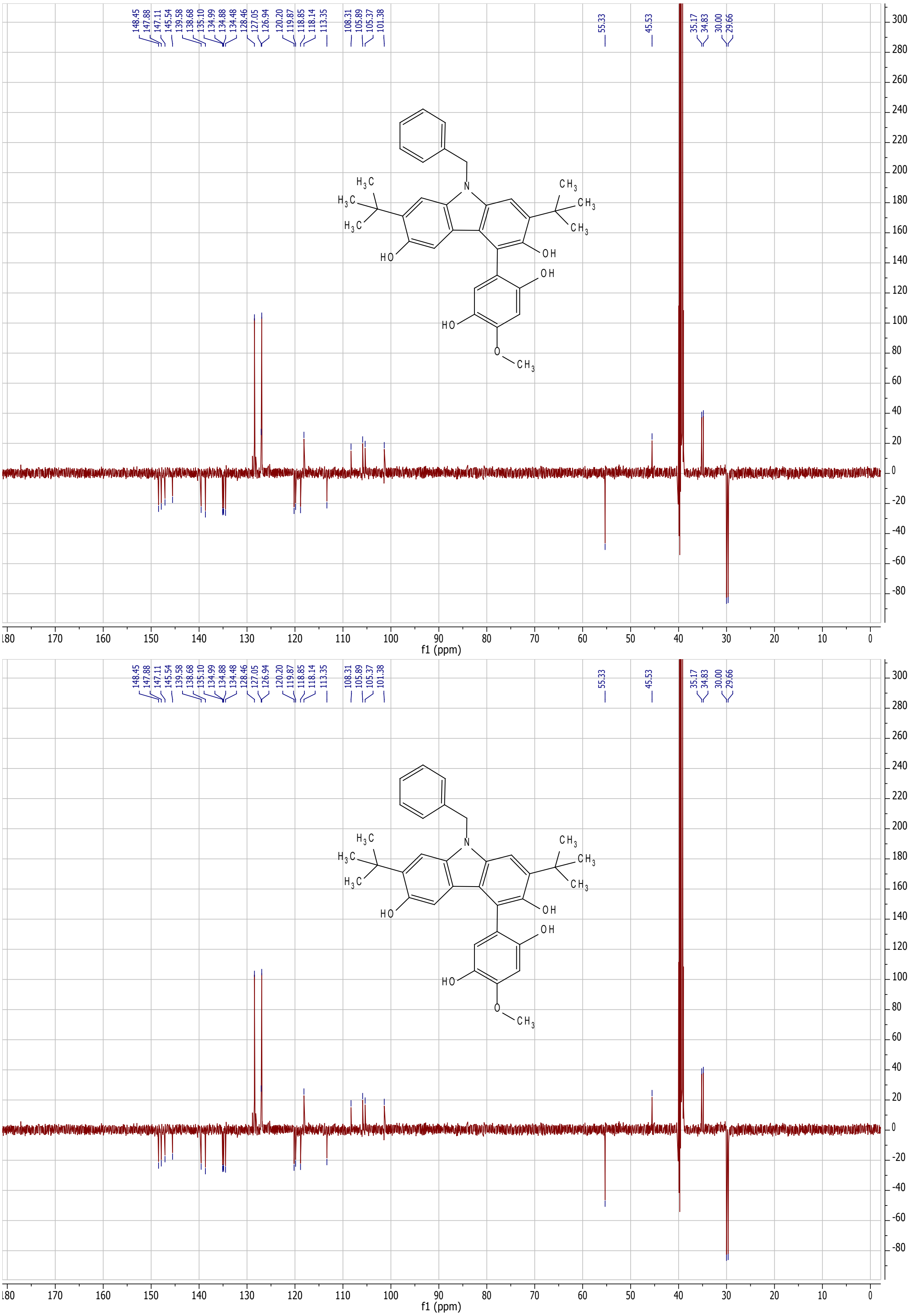

Fig. S3.7: ^{1}H and ^{13}C NMR spectra of compound **5**.

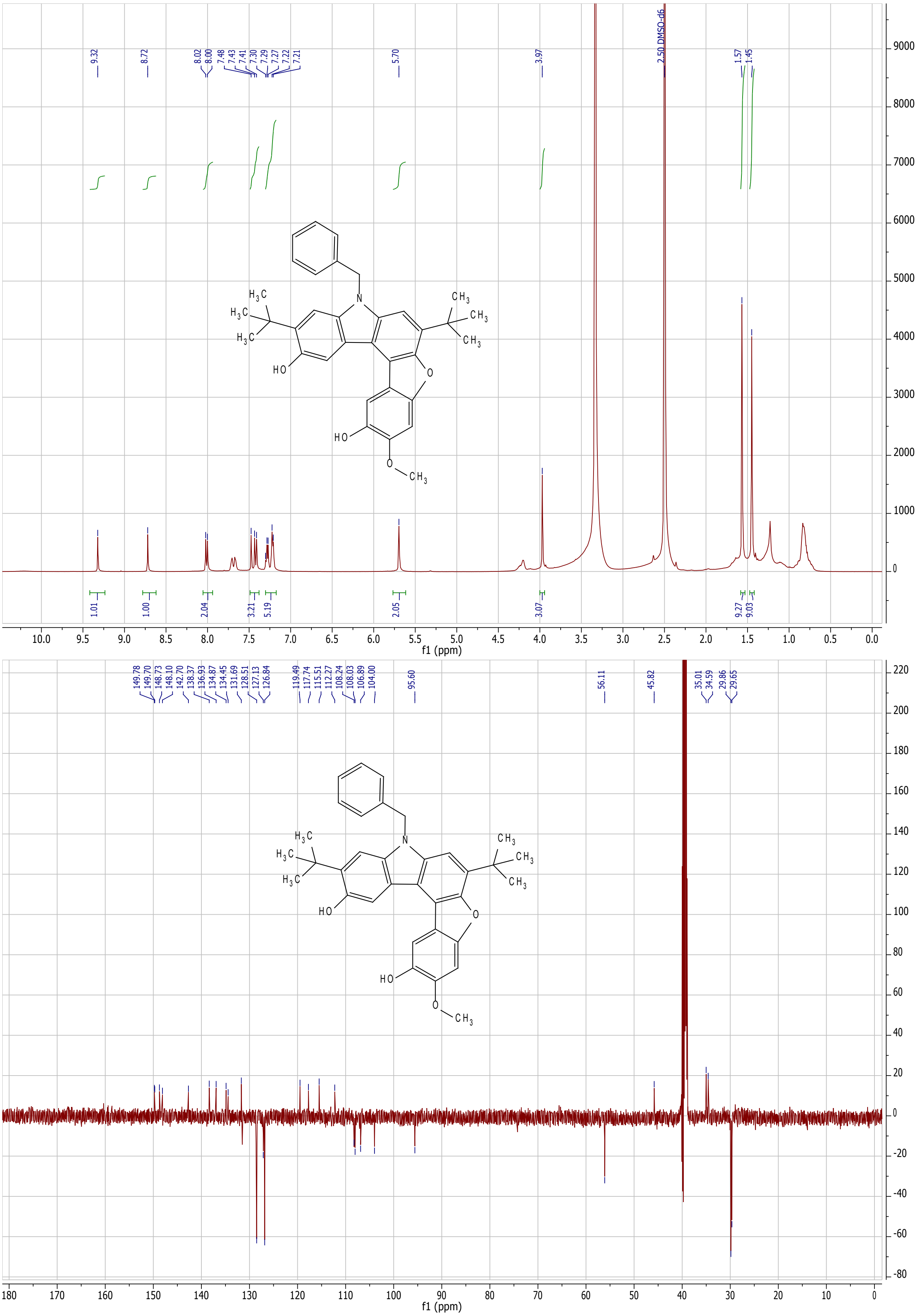

Fig. S3.8: ^{1}H and ^{13}C NMR spectra of compound **6**.

S4 NMR Assingments

4.1.1 NMR of Azatrioxa[8]circulene

In the following section the numbers for the five circulenes (2 in the manuscript) are designated **7**, **8**, **9**, **10** and **11** (Fig. S2).

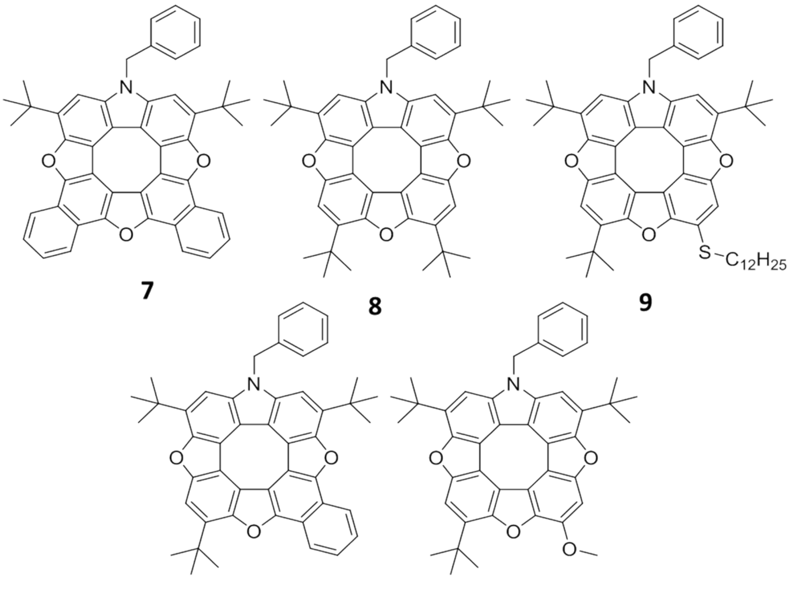

7 **8** **9** **10** **11**

Fig. S2 Structures of synthesized azatrioxa[8]circulene. Please note the numbers used in this section.

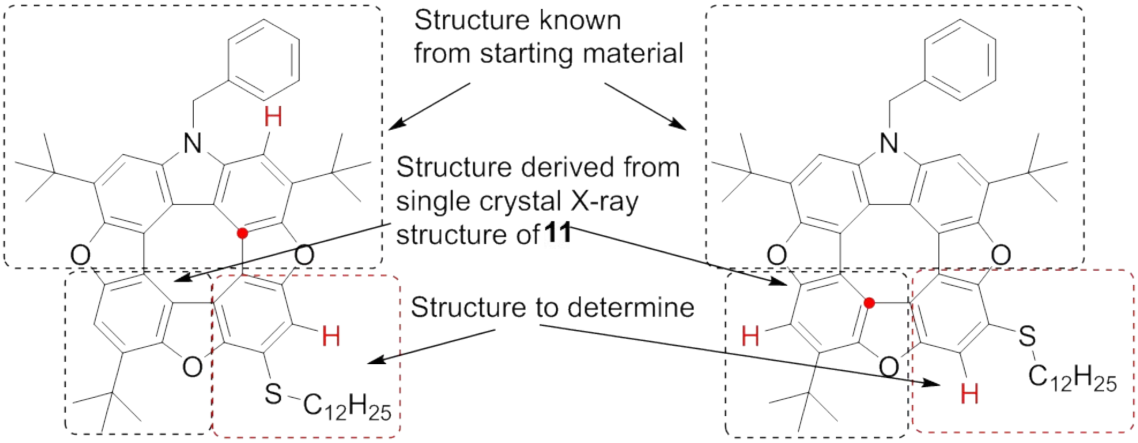

Fig. S3 Possible structures of azatrioxa[8]circulene $\mathbf{2}_{\mathbf{tBuSDO}}$ **(11)**. The ^4J-couplings to be observed by NMR spectroscopy are marked in red.

Multiple regio isomers are possible. However, from NMR it is seen that the isolated product is only one isomer. From the crystal structure of $\mathbf{2}_{\boldsymbol{t}\mathbf{Bu}\boldsymbol{t}\mathbf{Bu}}$ **(8)** it is evident how the 2-*tert*-butyl-1,4-benzoquinone reacts with the hydroxycarbazole. As this first step of the reaction is the same in the synthesis of mpl-tBu-SR, the position of the third *tert*-butyl group, can with a great certainty be transferred (Fig. S3). Using regular NMR techniques such as ^{1}H-NMR, ^{13}C-NMR, heteronuclear single quantum correlation (HSQC) and heteronuclear multiple-bond correlation (HMBC) spectroscopy, as well as more advanced techniques, a full assignment of the signals from the spectra to the molecule is possible. In addition to the regular techniques, non-decoupled ^{13}C-NMR and HMBC measured centered at a lower frequency long range coupling constant was used. This allowed the observation of the long range ^4J -couplings and from this observation it could be determined which isomer was isolated (Fig. S2). The following section will contain a description of the procedure to identify the structure of **11**.

4.1.1.1 NMR Analysis

All NMR spectra of azatrioxa[8]circulene **11** can be found below.

In the ^{1}H-NMR spectrum of **11** only one set of signals is present. From this it can be concluded that only one regioisomer has been isolated. Furthermore, the amount and integrals of signals match with the expected. The only part that is associated with some uncertainty is the signals from the C12-chain in the ^{1}H-NMR spectrum. The protons from the chain have very similar chemical shifts, as well as couplings that lead to split signals, and this leads to an area that is difficult to interpret. The overall integral matches with the expected and this area will, therefore, not be described further.

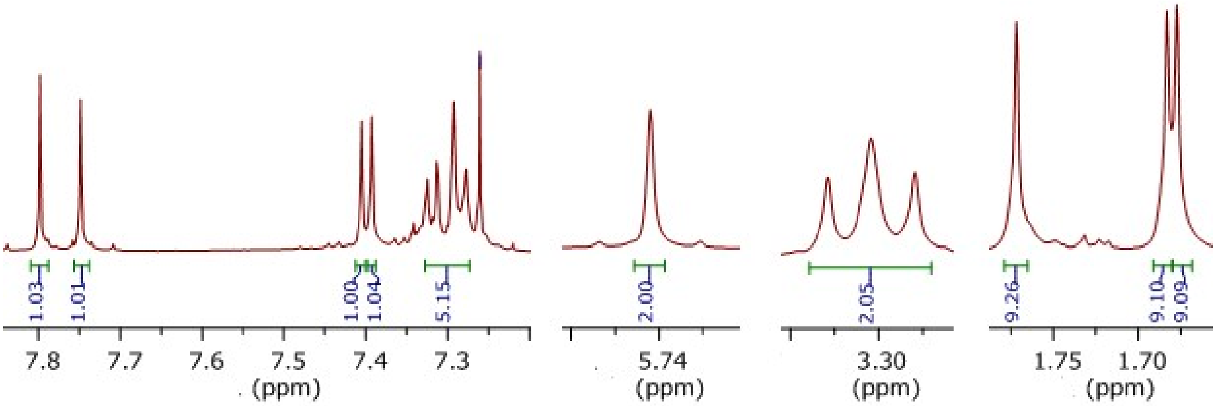

Fig. S4 Zoom of designated peaks in ^{1}H-NMR spectrum of azatrioxa[8]circulene **11**.

The aromatic area of the ^{1}H-NMR spectrum of **11** contains four singlets from circulene protons each integrating one, as well as signals from the benzene ring of the benzyl-group integrating five. At 5.74 ppm we find a singlet integrating two corresponding to the benzylic protons. A triplet integrating two at 3.30 ppm originates from the methylene-group attached directly to the sulfur atom. At 1.77, 1.68 and 1.67 we find three singlets integrating approx. nine each and these singlets originate from the three distinct *tert*-butyl groups (Fig. S4, Table S1). In the aliphatic area below 2 ppm the signals from the C12-chain are seen.

Table S1 Signals from the ^{1}H-NMR-spectrum. The terms for multiplicity are s = singlet, d = doublet, t = triplet, q = quartet and m = multiplet. A complete assignment of each signal can be found in Fig. S12.

	Chemical shift (ppm)	Integral	Multiplicity
A	7.80	1	S
B	7.74	1	S
C	7.40	1	S
D	7.39	1	S
E	7.35-7.27	5	M
F	5.75	2	S
G	3.30	2	t, $J = 7.4$
I	1.77	9	S
K	1.68	9	S
L	1.67	9	S

The correlation spectroscopy (COSY) spectrum of mpl-tBu-SR only reveals the couplings between the protons of the C-12 chain, and thereby gives no new information on the regiochemistry.

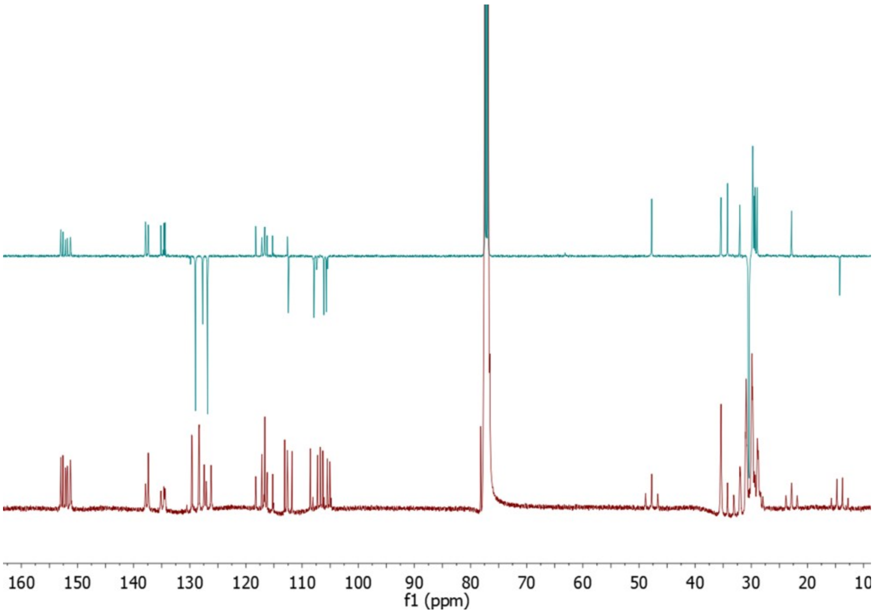

Fig. S5 ^{13}C-NMR of **11**. The top spectrum is an APT-spectrum and the lower spetrum is non decoupled.

The ^{13}C-NMR spectra (Fig. S5) are an APT-spectrum and a non-decoupled spectrum. In the ^{13}C-APT, signals from any carbon atom with zero or two protons bonded directly to it, will point in one direction (in this case upwards) and signals from any carbon atom with one or three protons bonded directly to it will point in the other direction (in this case downwards).

Table S2 Signals from the carbon spectra. The term dm stands for doublet of multiplets. Here a distinct doublet can be seen as the 1st coupling whilst the next couplings cannot be distinguished. Likewise tm stands for triplet of multiplets and qm stands for quartet of multiplets. A complete assignment of signals to structure can be found in Fig. e S12.

Aromatic area				**Aliphatic area**			
	Chemical shift (ppm)	Type of carbon	Multiplicity		Chemical shift (ppm)	Type of carbon	Multiplicity
1	153.0	C_q	d, J = 3.7 Hz	**29**	47.7	CH_2	tm, J = 136.8 Hz
2	152.6	C_q	d, J = 3.6 Hz	**30**	35.5	C_q/CH_2	M
3	152.1	C_q	d, J = 9.1 Hz	**31**	35.4	C_q/CH_2	M
4	151.8	C_q	d, J = 10.0 Hz	**32**	34.2	C_q/CH_2	tm, J = 145.7 Hz
5	151.3	C_q	d, J = 5.0 Hz	**33**	32.0	CH_2	tm, J = 140.0 Hz
6	151.2	C_q	d, J = 5.0 Hz	**34**	30.5	CH_3	M
7	137.9	C_q	m	**35**	30.4	CH_3	M
8	137.4	C_q	td, J = 3.7, 1.6 Hz	**36**	30.4	CH_3	M
9	137.4	C_q	td, J = 3.7, 1.6 Hz	**37**	29.9	C_q/CH_2	M
10	135.1	C_q	m	**38**	29.8	C_q/CH_2	M
11	134.6	C_q	m	**39**	29.8	C_q/CH_2	M
12	134.4	C_q	m	**40**	29.7	C_q/CH_2	M
13	129.0	CH	dd, J = 160.3, 7.3 Hz	**41**	29.7	C_q/CH_2	M
14	127.7	CH	dm, J = 160.4 Hz	**42**	29.7	C_q/CH_2	M
15	126.8	CH	dm, J = 157.5 Hz	**43**	29.5	C_q/CH_2	M
16	118.3	C_q	td, J = 3.9, 2.5 Hz	**44**	29.3	C_q/CH_2	M
17	117.2	C_q	d, J = 1.3 Hz	**45**	28.9	C_q/CH_2	M
18	116.7	C_q	m, J < 1.5 Hz	**46**	22.8	C_q/CH_2	tm, J = 126.0 Hz
19	116.7	C_q	m, J < 1.5 Hz	**47**	14.3	CH_3	qm, J = 124.1 Hz
20	116.6	C_q	m, J < 1.5 Hz				
21	116.2	C_q	d, J = 5.6 Hz				
22	115.3	C_q	d, J = 5.6 Hz				
23	112.6	C_q	d, J = 6.0 Hz				
24	112.6	C_q	d, J = 6.0 Hz				
25	112.4	CH	d, J = 165.4 Hz				
26	107.9	CH	d, J = 160.6 Hz				
27	106.1	CH	d, J = 157.4 Hz				
28	105.7	CH	d, J = 157.4 Hz				

In the aromatic area, 28 signals from carbon atoms should be present. Seven of these carbon atoms have one proton bonded (and thereby point downwards) whilst the remaining 21 carbon atoms have no hydrogen bonded (and thereby point upwards like $CDCl_3$). In the aliphatic area signals from 19 different carbon atoms should be present, four signals pointing down and 14 signals pointing up. This means that a signal is either missing, or lies at the exact chemical shift value as another signal. This can be determined by HSQC, or if no hydrogen atoms are attached, it can be determined by HMBC.

In non-decoupled ^{13}C-NMR spectroscopy the couplings between carbon atoms and hydrogen atoms are visible. Couplings between carbon atoms will exist (also in this case) but they will have an extremely low intensity, as only 1.1 % of the carbon atoms are NMR active. This means that the chance of a ^{13}C being bound to another ^{13}C is 0.012 %.

The magnitude of these carbon-hydrogen couplings in non-decoupled ^{13}C-NMR depends on the number of bonds between the atoms that couple. In aromatic compounds ^1J couplings are large in the range >150 Hz. In comparison ^2J and ^3J couplings are <20 Hz. ^2J couplings will typically be smaller than ^3J couplings. ^4J couplings are usually in the range 1 Hz or lower.[61] In Fig . S6, examples of each coupling are shown, and in table 4.02, the signals from the carbon spectrum are listed.

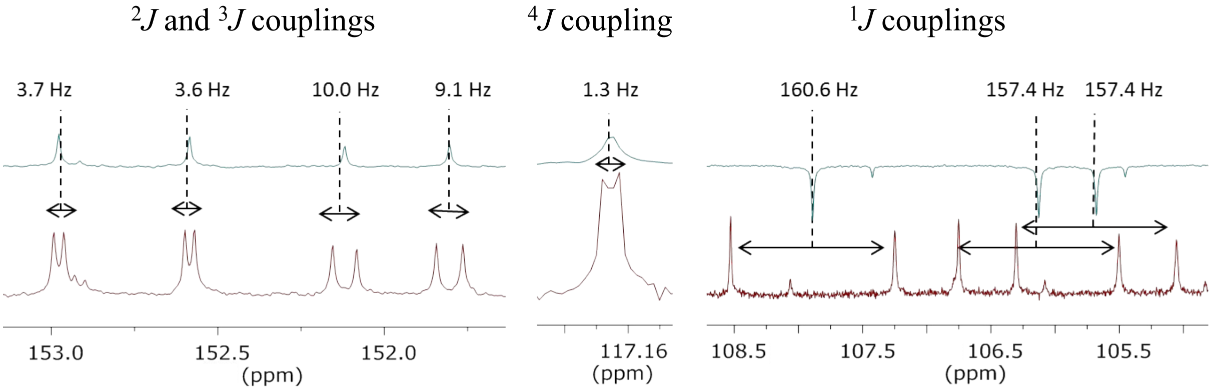
^2J and ^3J couplings

^4J coupling

^1J couplings

Fig. S6 Proton-carbon couplings in the ^{13}C-NMR spectrum. From the left: ^2J and ^3J couplings, ^4J coupling, ^1J couplings.

When HMBC spectra are recorded, a specific coupling frequency is targeted. The normal HMBC experiment uses a long range coupling constant centered at 5 Hz. This means that only couplings around this frequency will be observed. In the non-decoupled ^{13}C-NMR spectrum of mpl-tBu-SR we can determine the specific coupling constants of the ^{4}J-couplings we seek, and thereby change the parameters of the HMBC experiment. The signals in the carbon spectrum that only have 4J couplings are 17, 18, 19, and 20. Signals 18, 19, and 20 lie almost on top of each other, and are thereby indistinguishable in the 2D spectra.

From the HSQC and HMBC data (table S3) it is possible to assign the signals from the ^{1}H-NMR and ^{13}C-NMR spectra to the structure of azatrioxa[8]circulene **11**.

Table S3 Couplings in 2D spectra of mpl-tBu-SR. The dashed line (/) means or.

	HSQC	HMBC (5 Hz long range coupling constants)	HMBC (3 Hz long range coupling constants)
A	25	1/2/3/4, 21	2, 3, 16, 18/19/20
B	26	1/2/3/4, 22	1, 4, 17, 30
C	27	5/6, 8/9, 23/24	11/12, 18/19/20, 31
D	28	5/6, 8/9, 23/24	11/12, 18/19/20, 31
E	13,14,15	7, 13, 14, 29	15
F	29	8, 9, 15	
G	32	16	40, 43
H	34	10, 30	26
I	35/36	11/12, 31	28
J	35/36	11/12, 31	27

Numbers for carbons signals (table 4.02) and letters for hydrogen signals (table S3) will be used in this next part.

Starting from the benzylic position (**F**, **29**) - **F** couples with two quaternary carbons, **8** and **9**, as well as one carbon with a proton, **15**. The protons of **E** couple to the benzylic position, **29**, and this leads us to conclude that the protons from **E** as well as the carbons it couples to through HSQC **13**, **14** and **15** are part of the benzyl group. As **E** also couples to **7**, **7** must also belong to the benzyl group. **F** only couples to **15,** and therefore **15**, must be the signal from the carbon *ortho* to **F**. Integrals in the carbon spectrum are not reliable in the same way as in the proton spectrum. The integral of **13** is, however, twice that of **14**, therefore it is assumed that **13** is the signal from the carbon in the *meta* position to **F** and **14** is the signal from the carbon in the para position to **F**, giving the assignment shown in Fig . S7.

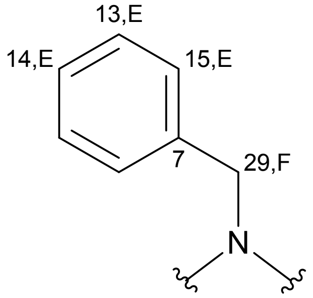

Fig. S7 Assignment of the benzyl group in azatrioxa[8]circulene **11**.

If we continue from the benzylic position (**F**,**29**) in the other direction of the nitrogen we had the coupling from **F** to **8** and **9**. These signals must originate from the quaternary carbon attached to nitrogen. As **C** (bonded to **27**) and **D** (bonded to **28**) couple with these carbons they must be ortho to **8** and **9**. **C** and **D** also couple to the following other carbon **5**/**6**, **23**/**24**, **11**/**12**, **18**/**19**/**20**. These signals must therefore also originate from the carbazole moiety of the circulene. As the protons from the *tert*-butyl groups **I** (bonded to **35**/**36**) and **J** (bonded to **35**/**36**) couple with **11**/ **12** this must be signals originating from the *tert*-butyl group on the carbazole moiety, and **11** and **12** the signals from the aromatic carbon attached directly to the *tert*-butyl group. **31** are the signals from the two aliphatic quaternary carbons from the *tert*-butyl groups lying at the same chemical shift value. This can be determined as **C** and **D** only couple to this aliphatic quaternary carbon in the HMBC. **18**/**19**/**20** only have ^{4}J-couplings in the non decoupled ^{13}C-spectrum indicating that they will be located with four bonds to the nearest proton. The positions of **5** and **6** and **23** and **24** can be determined from the assumption that the signals from carbon closest to heteroatoms will be the most downfield shifted. This means that **5** and **6** originate from the carbon attached to oxygen. This leads to the assignment of the carbazole moiety shown in Fig. S8.

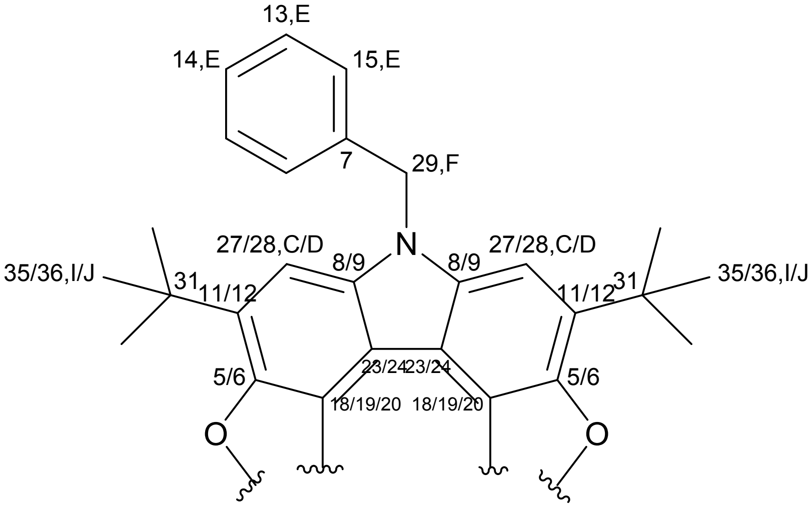

Fig. S8 Assignment of carbazole moiety in azatrioxa[8]circulene **11**.

The protons of the final *tert*-butyl group have the signals **H** (bonded to **34**). **H** couples with the quaternary carbon of the *tert*-butyl group **30**, the aromatic carbon with a proton attached **26** (bonded to **B**) and the quaternary aromatic carbon giving the signal **10**. From **B**, couplings to the following aromatic quaternary carbons are observed: **1**, **4**, **17** and **22**. The signal **17** originates from a position four bonds away from the nearest proton. If we again use the assumption that signals from carbon directly attached to heteroatoms, we find that **22** should come from the central eight-membered ring whilst **1** and **4** should originate from the carbon atoms next to the oxygen. The coupling constants of **1** and **4** are 3.7 Hz and 10.0 Hz respectively. With caution the coupling from **1** is assigned as a ^{2}J-coupling whilst that of **4** is assigned as ^{3}J-coupling giving the assignment seen in Fig .e S9.

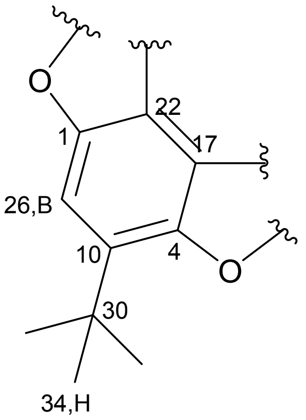

Fig. S9 Assignment of part of circulene azatrioxa[8]circulene **11**.

The final substructure, the aromatic thioether, must contain the proton giving the signal **A** (bonded to **25**). **A** couples to the following aromatic quaternary carbon: **2**, **3**, **16**, **18/19/20** and **21**. The protons from the methylene group giving the signal **G** (bonded to **32**) couples with **16** and the SR-chain must therefore be attached to this carbon. Signals **18/19/20** only have ^{4}J-couplings and are therefore positioned in the central eight membered ring accordingly. Again the assumption is that signals from carbon directly attached to heteroatoms are downfield shifted in comparison to other signals and we find that **21** must originate from a carbon atom in the central eight-membered ring whilst **2** and **3** come from carbon next to oxygen. The coupling constants of **2** and **3** are 3.6 and 9.1 Hz respectively and if the assumption that ^{2}J-couplings are generally smaller than ^{3}J-couplings is made once again, we can determine their positions. The assignment can be seen in Fig. S11.

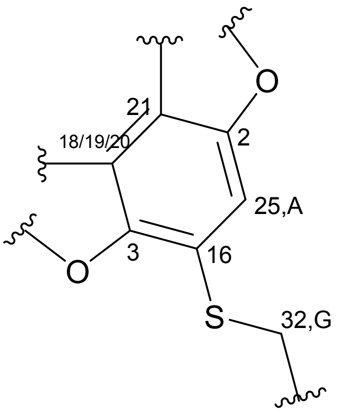

Fig. S11 Assignment of part of azatrioxa[8]circulene **11**.

As no coupling from **A** to **17** is present it is fair to conclude that the correct structure is the one shown in Fig. S12**.** There could, however, be couplings that are not visible in the obtained HMBC.

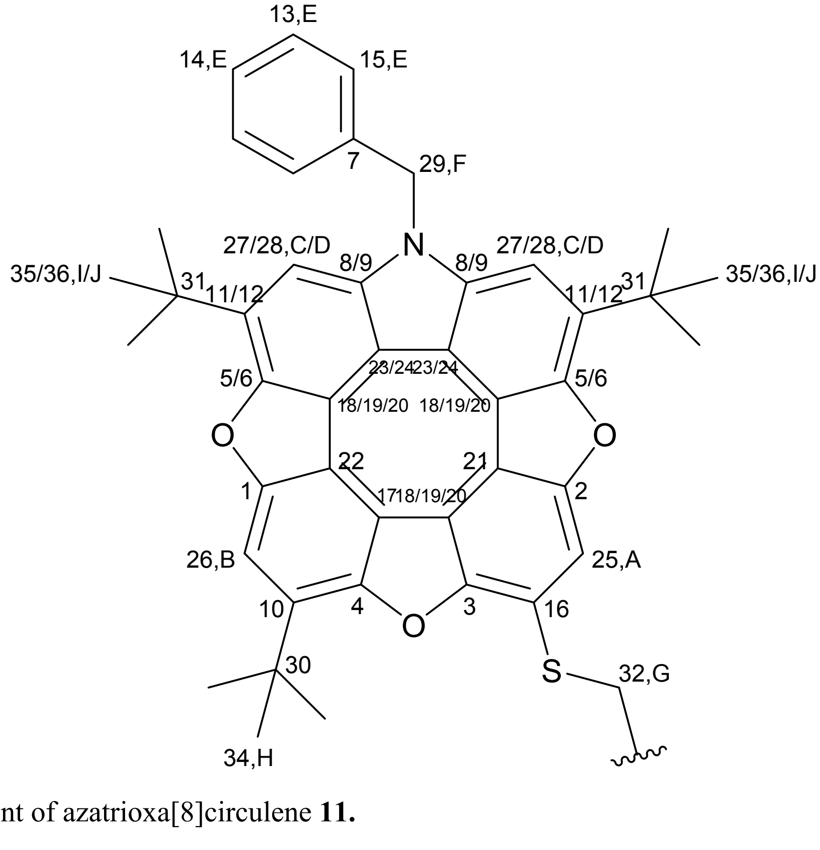

Fig. S12 Assignment of azatrioxa[8]circulene **11.**

4.1.2 Structure of Synthesized Azatrioxa[8]circulenes

From the crystal structure of **8** and the NMR-analysis of **11** important information of the reaction pathway of the circulene formation is obtained. As the other azatrioxa[8]circulenes synthesized are all either symmetric, or synthesized by adding 2-*tert*-butyl-1,4-benzoquinone in the first step, it is assumed that the third *tert*-butyl group ends up in a meta-position to the oxygen of the first furan ring formed. The NMR-analysis of **11** revealed that the thiododecyl group ends up in a meta-position to the other side of the carbazole moiety. From this, and from the fact that each synthesis gives rise to only one set of signals in the NMR spectra, it can be concluded that the azatrioxa[8]circulenes shown below, in fact represent the regioisomers obtained (Fig. S13).

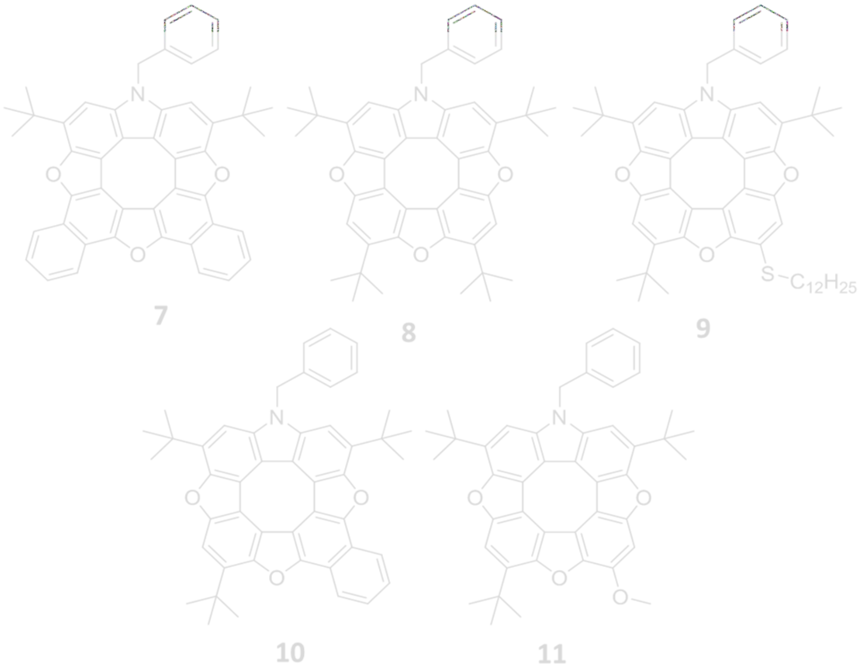

Fig. S13 Structures of synthesized azatrioxa[8]circulene.

S5 Electrochemical results

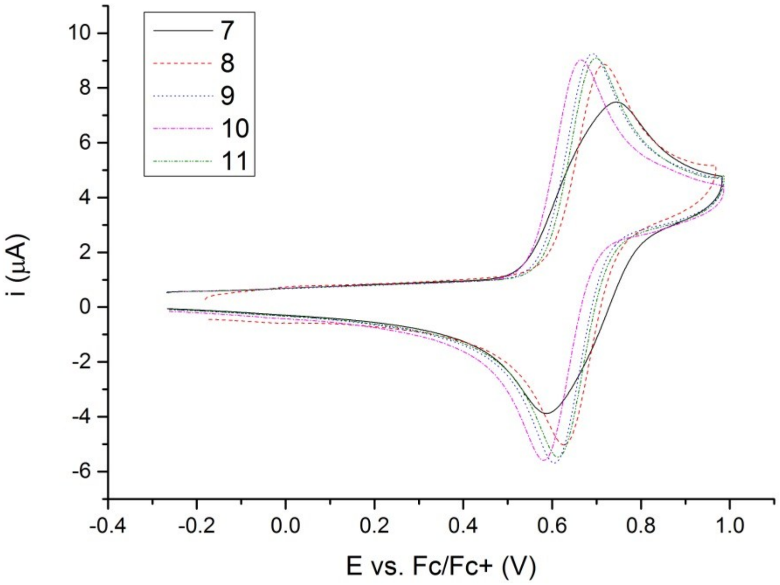

Fig. S14 Cyclic voltammograms for the 1st one-electron oxidation of the azatrioxa[8]circulenes.

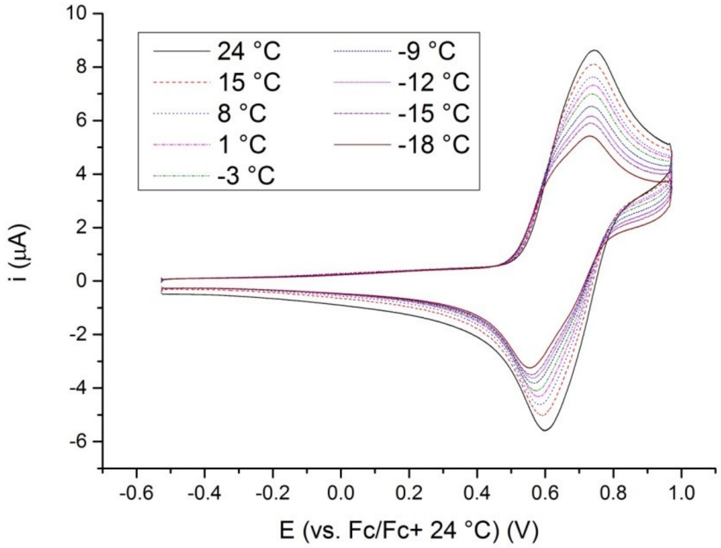

Fig. S15 Cyclic voltammograms for the 1st one-electron oxidation of azatrioxa[8]circulene **7** recorded at nine different temperatures. Solvent: CH_2Cl_2, concentration $5x10^{-4}$ mol L^{-1}, supporting electrolyte $(n\mathrm{Bu})_4NPF_6$ (0.1 M) working electrode: glassy carbon (*d* = 3mm), counter electrode: Pt, voltage sweep rate: 0.1 V s^{-1}.

.

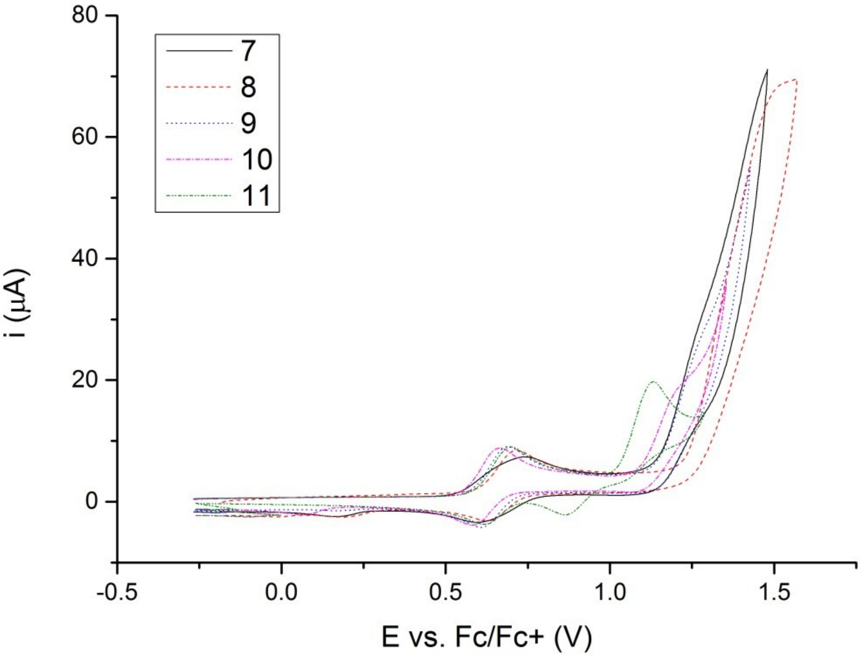

Fig. S16 Cyclic voltammograms including the 2nd oxidation of the five circulenes.

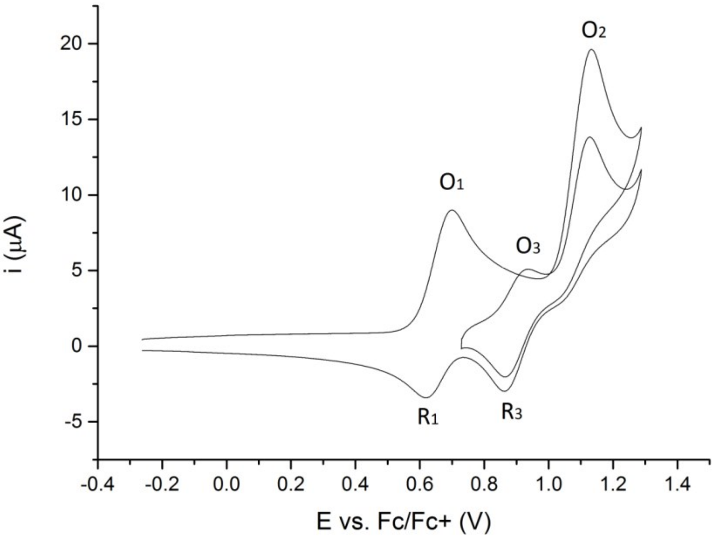

Fig. S17 Cyclic voltammogram for the the oxidation of azatrioxa[8]circulene **11**.

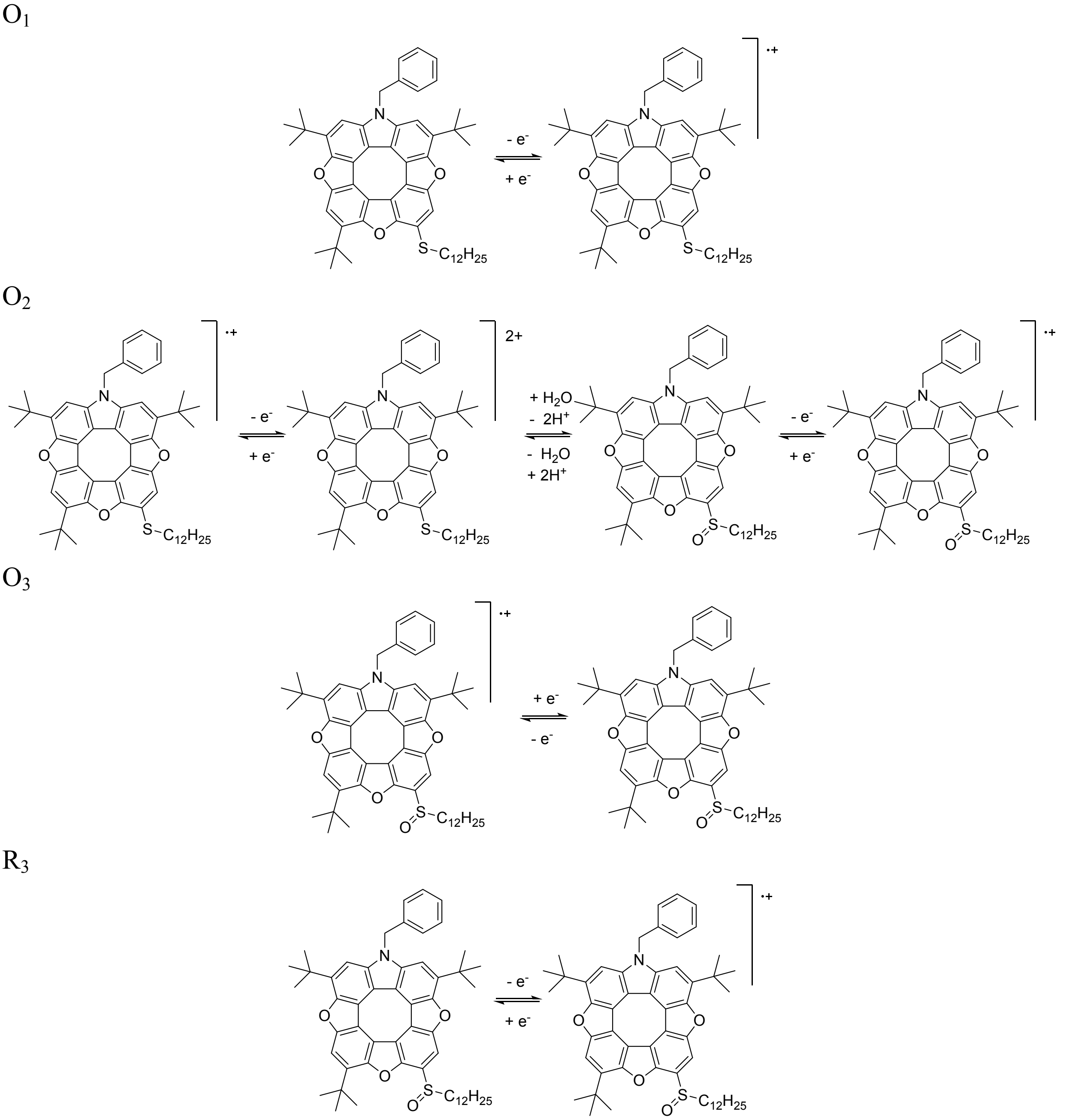

Assignment of the oxidation and reduction peaks in Fig. S17

Fig. S18 The electrochemical cell used for constant current oxidation of **11**. The dark color of the solution appeared upon oxidation.

Electrochemical preparation of the S-oxide of **11**. Azatrioxa[8]circulene **11** (25 mg) was subjected to constant current oxidation in the cell shown in Fig. S18. After the passage of charge corresponding to 1F (ox1), 2F (ox2), and 3F (ox3), a cyclic voltammetry experiment was carried in the electrochemical cell, and a small sample of the reaction mixture was collected for MALDI-TOF MS analysis (Fig. S19). After the passage of charge corresponding to oxidation by 3F the direction of the current was reversed and reduction was carried out corresponding to 1F (red4).

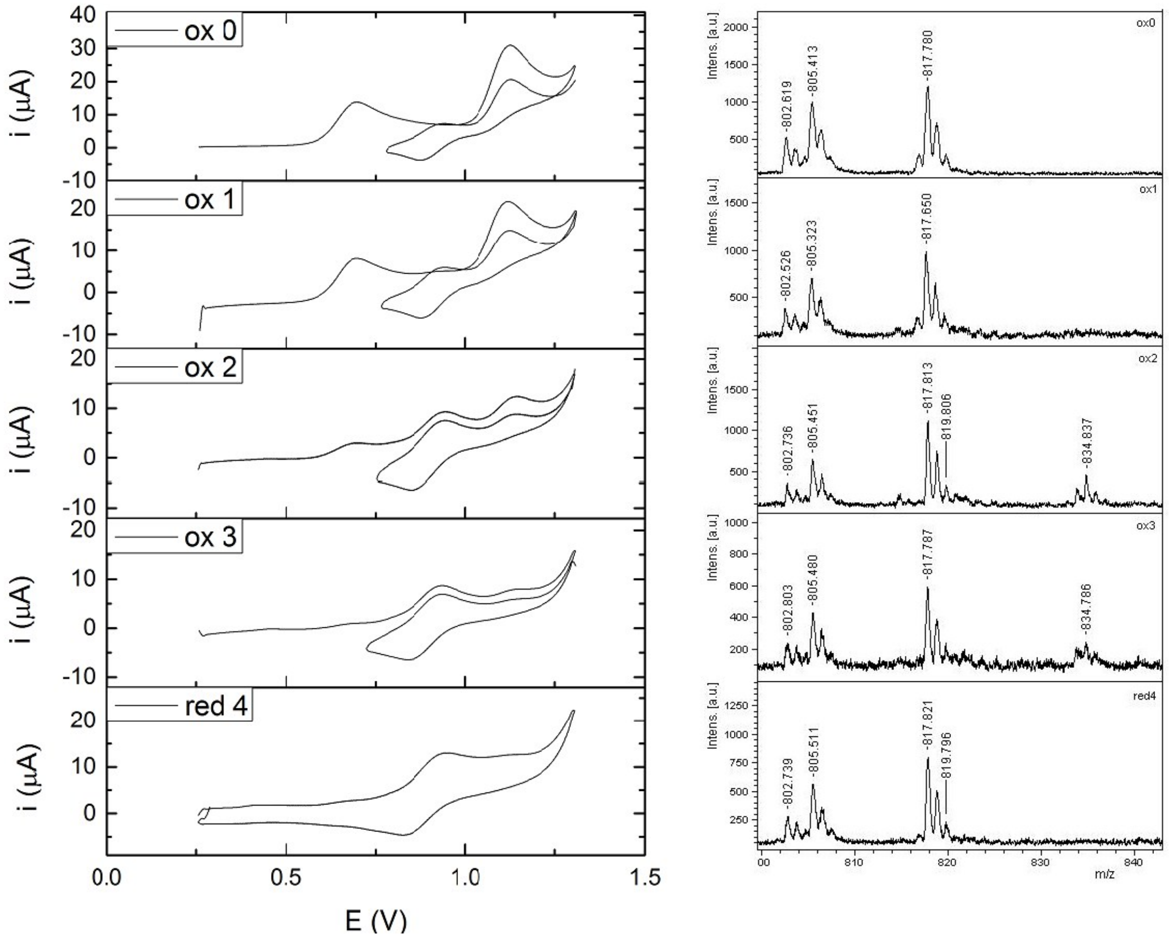

Fig. S19 Electrochemical oxidation of **11**. Cyclic voltammograms to the left were recorded directly in the preparative cell.

The MALDI-TOF MS revealed that a new compound with the mass of 834 g/mol was formed. This corresponds to $[M+1]^+$ of the sulfoxide of **11**. The MALDI-TOF MS spectra also indicate that some starting material is present even after the 3F oxidation. In order to obtain a better MALDI-TOF MS signal for of the sulfoxide of **11**, the reaction mixture was, after the final reduction, evaporated onto celite and filtered using dry column vacuum chromatography to remove the tetra-*n*-butyl ammonium hexafluorophosphate. This resulted in the spectrum shown in Fig. S20.

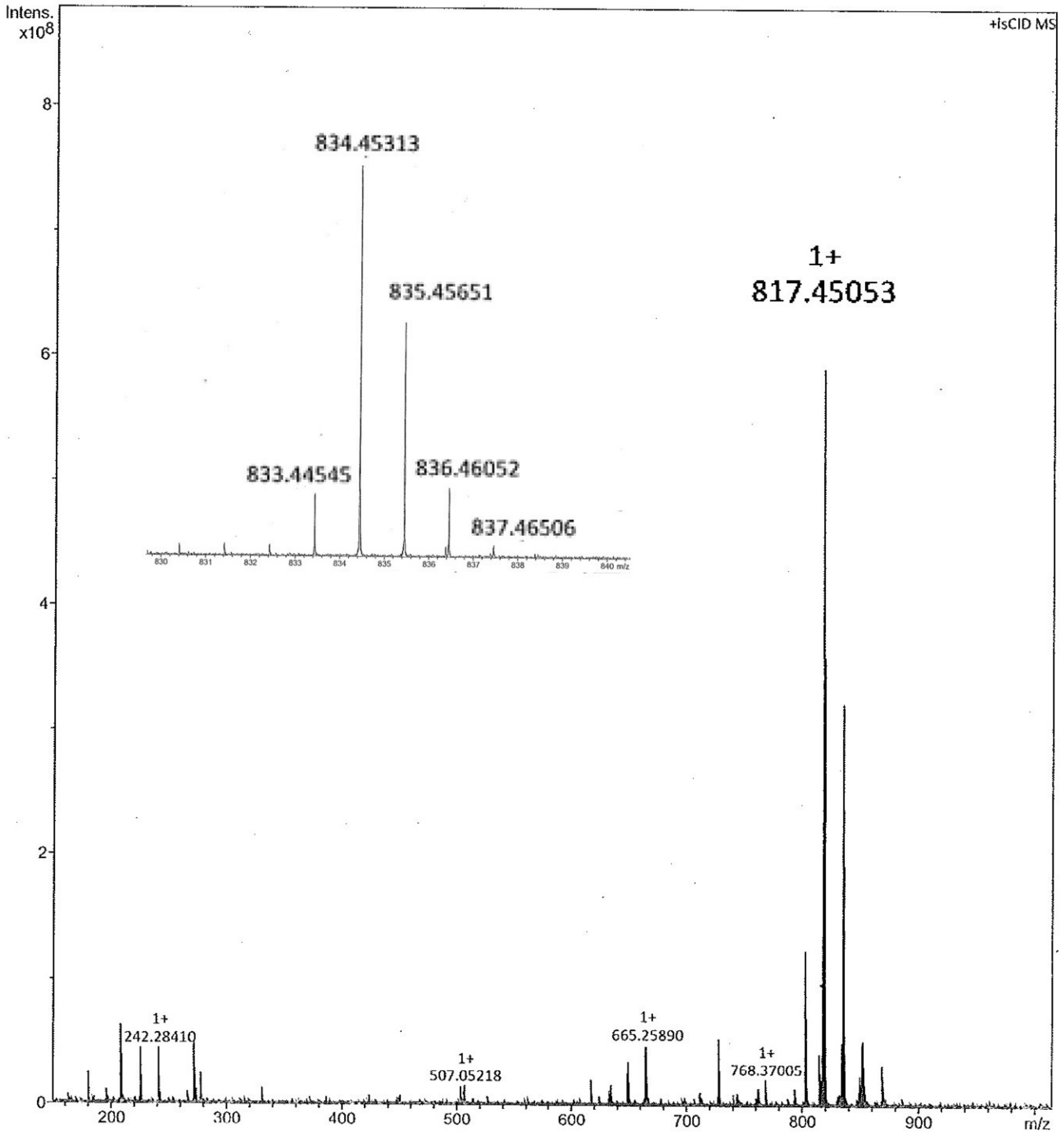

Fig. S20 MALDI HRMS of oxidized azatrioxa[8]circulenes **11** after column filtration.

S6 X-ray crystallography

Bond	X-ray	DFT[a]
a	1.428	1.431
b	1.399	1.398
c	1.430	1.435
d	1.401	1.405
e	1.432	1.435
f	1.402	1.401
g	1.392	1.402
h	1.387	1.401
i	1.388	1.416

Table 1: Selected experimental and calculated bond lengths of azatrioxa[8]circulene ($\mathbf{2}_{\mathbf{\mathit{t}Bu\mathit{t}Bu}}$) in Å. [a] DFT calculations performed using Gaussian 03 at the B3LYP/6-311+G** level of theory.

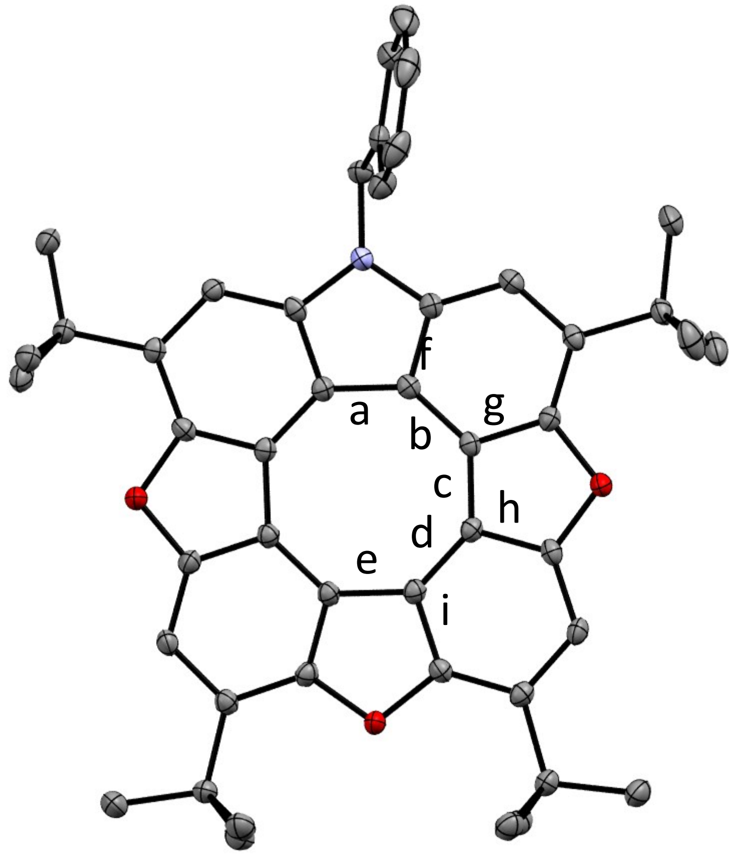

Fig. S21 Single crystal X-ray structure of $\mathbf{2}_{\mathbf{tButBu}}$.

$C_{47}H_{47}NO_3$; M =673.86; Monoclinic; a = 15.3940(17)Å, b = 13.3282(13)Å, c = 18.339(2)Å, α = 90°, β = 107.045(4), γ = 90°; V = 3597.4(7)Å^3; T = 122 K; space group P2$_1$/n ; Z = 4; μ(Mo-K_α) = 0.07 mm^{-1}; 87176 reflections measured, 7350 independent reflections (R_{int} = 0.092). The final R_1 value was 0.042 [$F^2 > 2\sigma(F^2)$]. The final R_1 value was 0.064 (all data). The final $wR(F^2)$ (all data) value was 0.106, The goodness of fit on F^2 was 1.01.